Monitoring in Situ Liver Metabolism in Rats Using Microdialysis. Comparison of Microdialysis Mass-Transport Model Predictions to Experimental Metabolite Generation Data

JULIE A. STENKEN,*,†,‡ LARS STÅHLE,|| CRAIG E. LUNTE,† AND MARYLEE Z. SOUTHARD§

Contribution from *Department of Chemistry and Center for Bioanalytical Research, University of Kansas, Lawrence, Kansas 66045-0046, Department of Chemical and Petroleum Engineering and Center for Drug Delivery Research, University of Kansas, Lawrence, Kansas 66045-2223, Department of Clinical Pharmacology, The Karolinska Institute, Huddinge University Hospital, SE–141 86 Huddinge, Sweden*

Received July 25, 1997. Final revised manuscript received December 17, 1997.
Accepted for publication December 18, 1997.

Abstract ☐ The generation of metabolites from two model compounds, phenacetin and acetaminophen, included in the perfusion fluid of a microdialysis probe implanted into rat liver was studied. When 60 μM phenacetin was included in the perfusion fluid using a flow rate of 1.0 μL/min, acetaminophen and acetaminophen sulfate were recovered at concentrations that ranged between 0.4 and 1.6 μM. Acetaminophen sulfate ($[AS]_{gain}$) diffused back into the microdialysis probe on a micromolar percentage basis of 8.9 ± 2.4% ($n = 3$) when acetaminophen was passed through the probe at a concentration between 11 and 12 μM. When 220–240 μM acetaminophen was passed through the probe, the percentage of acetaminophen sulfate recovered was 4.8 ± 1.4% ($n = 3$) ($P < 0.1$ compared to the 11 μM group). No acetaminophen glucuronide was detected in the dialysate samples. A mathematical model that describes mass transport in microdialysis sampling was used to predict the concentration of metabolite that could be recovered into the dialysate after the loss of a substrate compound that undergoes metabolism. The model predicts a metabolite recovery of 23.6% using estimates for phenacetin metabolism and 21.5% using estimates for acetaminophen metabolism. The results presented here indicate that microdialysis has potential to be used to study local in situ metabolism and with further refinements of the microdialysis mass-transport model may be used to estimate in vivo metabolic formation rates.

Introduction

Microdialysis is a well-known method for obtaining protein-free samples from the extracellular fluid (ECF) space of brain and has allowed many researchers to study neurochemistry in localized brain regions.[1,2] Microdialysis has also been used as a method to sample the ECF of other tissues[3] including the liver.[4–7] Analytes that diffuse freely in the ECF to or from the implanted microdialysis probe can be sampled. The efficiency of this diffusive process in microdialysis is called recovery and is defined in eq 1.[8]

$$E_d = \text{Recovery} = \frac{C_{outlet} - C_{inlet}}{C_{\infty ECF} - C_{inlet}} \quad (1)$$

The values of the inlet concentration, C_{inlet}, the outlet concentration, C_{outlet}, and the far-field concentration, $C_{\infty ECF}$, may vary depending upon the physiological and pharmacological conditions and the type of experiment that is being performed. When microdialysis is used to sample neurotransmitters such as dopamine, then $C_{inlet} = 0$ and $C_{\infty ECF}$ equals a finite number. Since diffusion across the membrane and in the tissue is symmetric to and from the probe, it is possible to use microdialysis to locally administer a compound by including it in the perfusion fluid. In this case, C_{inlet} would be the concentration of the included compound and $C_{\infty ECF}$ would be zero.[9]

One of the principal advantages of using microdialysis is the small size of the dialysis membrane and cannula. A microdialysis probe can be placed into a distinct tissue region because the outer diameter of the dialysis membrane is between 220 and 500 μm. This allows for the study of localized metabolic events in a specific tissue region using microdialysis.

A few research groups have compared microdialysis results with mathematical models. Microdialysis sampling coupled with the use of a mathematical model that described transport to and from microdialysis probes derived by Bungay et al.[10] and Morrison et al.[11] has been used to study ziduvodine (AZT) transport in rat brain.[12] Additionally, a mathematical model has been used in the study of localized muscle blood flow in rats.[13] The blood flow through the tissue was determined by correlation of the experimental results with a mathematical model that describes the loss of ethanol to the tissue space based upon diffusion of ethanol from the microdialysis probe and its uptake into the capillaries. Capillary uptake of ethanol is dependent upon blood flow rate and the experimental data showing this result has been published.[14]

This paper describes the use of microdialysis sampling coupled with a previously developed mathematical model[15] to interpret experimental metabolism data obtained from liver microdialysis experiments in which phenacetin and acetaminophen were included in the perfusion fluid. The development of a mathematical model that predicts the concentration of metabolites formed after a local infusion of a substrate requires a consideration of the multitude of physiological processes that occur in the liver. The liver is a highly perfused organ which is organized via an acinar structure.[16,17] The blood flow through the liver occurs through blood spaces originating from the portal vein (75%) and hepatic artery (25%).[18] Blood from both inlets flows through these spaces, which are called sinusoids, and is combined at the outlet into the hepatic vein. The hepatocytes are aligned along the sinusoids in a one-unit layer of cells. The drug-metabolizing activity of the liver varies through three separate regions which are segregated into zones (one, two, or three) and is dependent upon the oxygen

* Corresponding author. Phone: (518) 276-2045. Fax: (518) 276-4887. E-mail: Stenkj@rpi.edu.
† Department of Chemistry and Center for Bioanalytical Research, University of Kansas.
‡ Present address: Department of Chemistry, Rensselaer Polytechnic Institute, Troy, NY 12180-3590.
§ Department of Chemical and Petroleum Engineering and Center for Drug Delivery Research, University of Kansas.
|| Huddinge University Hospital.

S0022-3549(97)00288-8 CCC: $15.00 Published on Web 02/05/1998

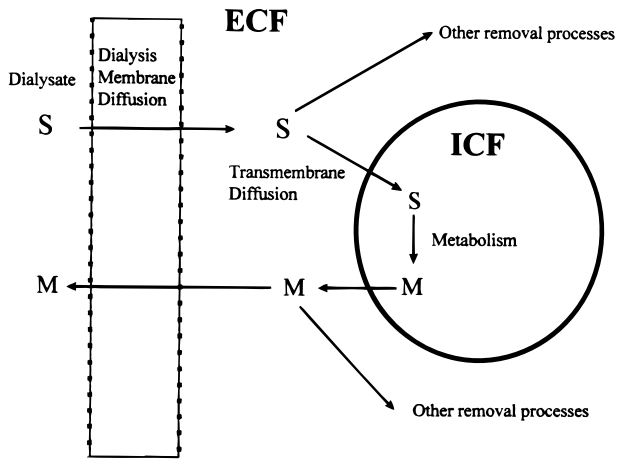

Figure 1—A schematic diagram illustrating the pathway that a substrate must pass from the microdialysis probe to the tissue space. The substrate must diffuse through the dialysis membrane and the cell lipid bilayer prior to metabolism. The metabolites must diffuse back through the lipid bilayer and through the probe dialysis membrane prior to analysis.

gradient through these zones.[19] Zone 1 is the closest to the entry of the periportal region (where the hepatic artery and portal vein enter the liver), zone 2 is in the middle, and zone 3 is closest to the exit, which is the perihepatic region. Between the sinusoids and the hepatocytes lies the space of Disse, which allows for equilibrative exchange between the sinusoid and the hepatocytes.

Most drugs form different metabolites after a dose is given. This known result indicates clearly that drug-metabolizing enzymes within the liver act concurrently. Therefore, the complexity of xenobiotic metabolism cannot be completely understood in vivo from individual in vitro studies of single drug-metabolizing enzymes.[20] The extent of drug metabolism in the liver has often been studied using the isolated perfused liver technique.[21] Different models have been developed to predict metabolite formation based on blood flow patterns in the liver.[22]

In the experiments described here, phenacetin and acetaminophen were included in the microdialysis perfusion fluid at a known concentration and are used as substrates to be metabolized in the liver. The microdialysis probe may be thought of as an artificial blood vessel which allows diffusive exchange across its semipermeable wall.[2] The direction of transport of the drug and metabolite are opposite that in the liver perfusion studies. Here we are putting the hepatocytes in direct contact with the substrate. Enzymatic heterogeneity still exists, but will now depend on the probe implantation site, rather than the length down the sinusoid. Since the probe is much wider (500 μm) and longer (4 mm) than the acinus (300 μm), it is reasonable to consider this situation a well-stirred case and assume that enzymes are randomly spaced around the microdialysis probe.

A substrate gets metabolized only after it diffuses through the dialysis membrane into the ECF and through the cell membrane of the hepatocyte in order to reach the metabolic enzymes found inside the hepatocyte as illustrated in Figure 1. Phenacetin is oxidized to acetaminophen via an *O*-deethylation catalyzed by cytochrome P450, CYP1A2, which accounts for 80−90% of its metabolism.[23] Acetaminophen can be sulfated, glucuronidated, or oxidized to the quinoneimine.[24] Sulfation of phenolic substrates occurs via high-affinity, low-capacity cytosolic sulfotransferase enzymes, which have an estimated reported whole liver in vivo V_{max} value of 500 nmol min^{-1} per liver and a K_m of 10 μM.[18] Glucuronidation of phenolic substrates occurs via the glucuronyltransferases, which are located in the endoplasmic reticulum of the hepatocytes and have an estimated whole liver in vivo V_{max} of 1000 nmol min^{-1} per liver and a K_m of 200 μM.[18] The minor metabolites of phenacetin metabolism include phenetidine, which occurs via a deacetylation reaction; 2-hydroxyphenacetin, which is an aromatic hydroxylation product; and 3-([5-acetamido-2-hydroxyphenyl)thio]alanine, which is the cysteine conjugate of acetaminophen.[23] The concentration of these minor metabolites was not measured in these experiments.

Prediction of the concentration of metabolite (C_{dial}) that returns to the microdialysis probe after metabolism of a substrate requires metabolite kinetics to be incorporated into a previously developed mathematical model.[15] Here, we use a model we have previously developed based on the work of Bungay et al. and Morrison et al.[10,11] The experimental results are compared with predictions calculated using this theoretical model that predicts metabolite back-extraction into the microdialysis probe. Although several groups have used mathematical models to describe microdialysis recovery[10,11,13] and others have studied in situ liver metabolism,[4,5,25] there have been no applications of a theoretical model to describe metabolite back-extraction in microdialysis sampling.

Materials and Methods

Theory—A concentration profile of the substrate calculated at different radial points is the first step to modeling metabolite return into a microdialysis probe. We have recently shown how a developed finite-difference model can be used to calculate concentration profiles in liver[15] on the basis of the work of Bungay[10] and Morrison.[11] The substrate concentration profile is needed to calculate the metabolite concentration profile. Once the metabolite concentration profile is calculated, then the concentration of the metabolite that diffuses into the probe can be calculated.

Substrate Concentration Profile—*ECF*—All analytes that are either sampled or delivered via the microdialysis probe will diffuse through the extracellular fluid space (ECF) of the tissue in which the microdialysis probe is implanted. In addition to diffusion, kinetic processes such as uptake, metabolism, and capillary permeability will remove the analyte from the ECF in the tissue. The transient concentration time profile for this process is described by eq 2.

$$\frac{\partial C_{ECF}(r,t)}{\partial t} = \Phi_{ECF} D_{ECF} \frac{1}{r} \frac{\partial}{\partial r}\left(r\left(\frac{\partial C_{ECF}(r,t)}{\partial r}\right)\right) - \Phi_{ECF} k_L C_{ECF}(r,t) \quad (2)$$

Equation 2 accounts for the diffusive (D_{ECF}, cm^2/min) and kinetic processes that occur in the tissue space. For simplicity k_L (min^{-1}) is used, where k_L is a lumped kinetic rate constant that includes the summation of rate constants for tissue metabolism (k_m), exchange between the intracellular and extracellular space (k_{ei}, k_{ie}), or permeation across capillary walls (k_{ep}), and r (cm) is the radial distance from the probe. Φ_{ECF} is the aqueous volume fraction of the tissue space and is used in this equation to remind the reader that diffusion is assumed to occur only in the ECF water space. In the solved mathematical model k_L is subdivided into the individual kinetic processes mentioned above such as metabolism, capillary permeation, or uptake.[26] The z axis (length of the probe) is averaged in the final numerical solution and is therefore not included in the above partial differential equation. The extent of tissue binding for acetaminophen and phenacetin in the liver is an unknown quantity and it has not been included in the model formulation. A partition coefficient between the ECF and ICF is assumed to be unity.

Equation 2 does not account for convection around the microdialysis probe. Inclusion of convection into the diffusion model adds much complexity to the modeling process. The possibility of convection around the probe exists especially in a tissue such as the liver, where the respiration of the rat moves the liver. The volumetric flow rate of any convection and whether the convection process has laminar flow are difficult parameters to obtain in vivo.

Membrane—In the membrane, only diffusion (D_{mem}, cm²/min) is allowed to occur. An effective diffusion coefficient is used that takes into account diffusion through the membrane pores and polymer. For most dialysis membranes, it is reasonable to assume that the majority of the mass transport occurs through the water space within the membrane pores. Diffusion through the water space in the pores provides less resistance to mass transport than polymer diffusion. The mass balance for the substrate in the membrane becomes

$$\frac{\partial C_{mem}(r,t)}{\partial t} = \Phi_{mem} D_{mem} \frac{1}{r} \frac{\partial}{\partial r}\left(r\left(\frac{\partial C_{mem}(r,t)}{\partial r}\right)\right) \quad (3)$$

where Φ_m and D_m are the membrane volume fraction and diffusion coefficient, respectively.

Dialysate—Finally transport in the dialysate must be accounted for by

$$\frac{\partial \overline{C_d}}{\partial t} = Q_d \frac{\partial \overline{C_d}(r,t)}{\partial z} - 2\pi r_i D_{mem} \Phi_{mem} \frac{\partial C_{mem}(r_i,z)}{\partial r} \quad (4)$$

where $\overline{C_d}$ is the averaged substrate concentration in the dialysate and z is the axial position along the probe in the direction of flow, Q_d is the dialysate flow rate (μL/min), r_i is the inner membrane radius (cm), and Φ_m is the volume fraction of the membrane since it is assumed that transport primarily occurs through membrane pores.

Metabolite Concentration Profile—A metabolite generation term is needed to obtain the metabolite concentration profile in the tissue space. This term is shown below in eq 5

$$G_{ICF} = k_{m,sub} C_{ICF,sub}(r) \quad (5)$$

where $C_{ICF,sub}(r)$ is the concentration for the substrate predicted by the model for a particular radial point, r, and $k_{m,sub}$ is the metabolic rate constant for the degradation of the substrate. The mass balance of the metabolite in the tissue space then becomes

$$\frac{\partial C_{ECF,met}(r,t)}{\partial t} = \Phi_{ECF} D_{ECF,met} \frac{1}{r} \frac{\partial}{\partial r}\left(r \frac{dC_{ECF,met}(r,t)}{dr}\right) + \Phi_{ICF} G_{ICF}(r) - \Phi_{ECF} k_{L,met} C_{ECF,met}(r,t) \quad (6)$$

Note that $D_{ECF,met}$ and $k_{L,met}$ for the metabolite may be different than the values for the substrate.

Boundary Conditions and Numerical Solution—The metabolite model solution requires the substrate concentration to be at a steady-state. The program then calculates the metabolite concentration using the same mass balance equations listed above along with the boundary conditions listed below for the substrate concentration. A second assumption made is that a rapid equilibrium exists for both substrate and metabolite between the ECF and the intracellular fluid space (ICF) as was used by Morrison et al.[11]

$$J_{mem} = J_{ECF} \qquad D_{mem}\Phi_{mem} \frac{\partial C_{mem}}{\partial r} = D_{ECF}\Phi_{ECF} \frac{\partial C_{ECF}}{\partial r} \quad (7)$$

The following boundary conditions were used to obtain the solution to the equations. The far-field concentration, $C_{\infty ECF}$, is zero since the nonendogenous substrate is delivered to the tissue space by inclusion in the perfusion fluid. This is a reasonable assumption since the concentration will be highest near the probe membrane and will drop exponentially farther from the probe because of kinetic processes such as metabolism and capillary permeation that remove substrate from the tissue. The inlet dialysate concentration is known. It is assumed that substrate concentrations outside the probe are lower than inside the probe because the tissue has kinetic processes that remove the substrate in addition to diffusion, whereas in the dialysate and membrane no kinetic processes occur. The conservation of flux across the membrane/ECF interface is defined in eq 7. Φ_m is included in eq 7 because it is possible that diffusion can occur though the polymer. Flux must be conserved between the membrane and the dialysate which is defined in eq 8.[10]

$$D_{mem}\Phi_{mem} \frac{dC}{dr}(r,t)|_{r_i} = \frac{D_d[C_{mem} - \overline{C_d}]}{r_i - r_c}\left(\frac{35}{13}\right) \quad (8)$$

In eq 8 the term $D_d/(r_i - r_c)$ (r_c is the inner cannula radius) has the same form as a mass transfer coefficient and can then be used to relate membrane and dialysis flux in the model as was shown by Bungay et al. for their steady-state model (see eq A1 in their paper).[10]

Equations 2−4 are solved simultaneously using the boundary conditions listed above at various time points by using a developed FORTRAN program to obtain the substrate concentration exiting the probe and the substrate concentration profile away from the probe.[28] The partial differential equations which describe the mass balances in the dialysate, the membrane, and the tissue are solved by using an implicit finite-difference scheme which can be found in a numerical methods textbook.[27] For this numerical model, an initial guess must be made for the concentration of the dialysate, and the program uses a relaxation technique to reach the final answer.[28]

After calculating the steady-state substrate concentration profile, the concentration of the metabolite in the ICF is calculated by using eq 5. With this calculation the metabolite concentration in the dialysate can be found by using eqs 3, 4, and 6. It is possible to solve this model transiently to predict the outlet concentration, C_{outlet}, of the substrate and metabolite at each time point. Calculation of transient C_{outlet} for the substrate and metabolite would increase computation time and is not the focus of this paper, since the experiments performed here were steady-state.

Linear Kinetics Assumptions—The model to predict the substrate concentration profile is based on linear kinetics. The reasoning behind using linear kinetics is multifold. Although most biologically relevant rates are saturable, they can be approximated as first-order rates by assuming the substrate concentration is low enough that it reduces the Michaelis−Menten equation to a first-order equation.[29] The more important modeling reason is that incorporation of nonlinear kinetics into the mass-balance equations (2 or 6) adds much complexity to the coding and implementing of the computational solution. The task of incorporating the nonlinear kinetics into the mathematical model is important and is ongoing in our laboratories. Finally, although it is intuitively expected that nonlinear kinetics would affect E_d, i.e., by lowering E_d as the concentration of the substrate leaving the probe becomes greater than K_m, in the liver there are multiple kinetic processes that affect the removal of compounds from the microdialysis probe. In particular, the effect of capillary permeability has been shown to have a much greater influence on the E_d than metabolism, even when metabolic processes are inhibited. Keeping this in mind, error in the prediction of E_d will occur for any substrate concentration greater than the enzymatic K_m that describes the removal of a substrate, but this error will be low because of the large capillary permeability, k_{ep}, in the liver that dominates the kinetic removal of substances in the liver, as was shown in ref 15. However, this argument will most likely not hold for E_d predictions with saturable kinetics in tissues such as the brain or the skin, where the capillary permeation rate constant, k_{ep}, is much lower than in the liver.

Michaelis−Menten Kinetics—Two versions of the model program that calculate the concentration of the metabolite entering the probe have been coded with different assumptions. The first assumes that metabolism rate constants for the generation term described in eq 5 are linear. The second model uses Michaelis−Menten kinetics in the generation term. This is not as arduous a task to code as in the first model case that predicts the substrate C_{outlet}. In this second model program, the Michaelis−Menten terms are included in a separate matrix and are simply multiplied by the parent concentration found by model program 1. In this case, the computer program calculates the $C_{ECF,met}$ in each radial space based on the Michaelis−Menten kinetic terms and the value calculated for the substrate concentration, $C_{ECF,sub}$. This is not possible in the first program since the computer must calculate the $C_{ECF,sub}$ and that would require extensive iteration at each radial step since a Michaelis−Menten kinetic term would include $C_{ECF,sub}$ in the denominator.

Modeling Parameter Choice—The rationale for choosing the aqueous diffusion coefficient values (D_d) for phenacetin and acetaminophen has been previously described.[15] To find D_{ECF} corrected for tortuosity in the tissue space, D_d was divided by the

Table 1—Values Used for Model Analysis of Metabolite Generation

inner radius (cm) (r_i)	0.020
outer radius (cm) (r_o)	0.025
estimated (D_d) (cm^2/s)	7.5×10^{-6}
estimate membrane (cm^2/s) (D_m)	1.5×10^{-6}
estimate extracellular fluid D_{ECF} with tortuosity included	3.3×10^{-6}
volume fraction of liver ECF (Φ_{ECF})	0.2
estimated (ICF) (min^{-1}) (k_m) [phenacetin → APAP]	1.8[a]
estimated (ICF) (min^{-1}) (k_m)[APAP → APAP-SO_4]	5.0[a]
estimated (ICF) (min^{-1}) (k_m)[APAP → APAP-glucuronide]	0.5[a]
estimataed rate of ECF/plasma exchange (min^{-1}) (k_{ep})[capillary exchange]	2.0
membrane length (mm)	4.0
flow rate of dialysate (mL/min) (Q)	1.0

[a] The first-order kinetic rate constants were determined as listed in the methods section of the text.

tortuosity of the tissue space, which has been suggested to be 2.25 for brain tissue.[30] A tortuosity value for liver tissue has not been reported, but was assumed to be 2.25. The volume fraction of the liver is reported to be approximately 0.2.[17]

The tortuosity of the tissue increases the relative aqueous diffusion coefficient of any analyte by increasing the path length that an analyte must travel. Although tortuosity and liver volume are difficult to measure, they are important parameters to consider for any in vivo diffusion process.[31] It is the tortuosity and volume fraction in the in vivo tissue which makes it difficult to compare results to an in vitro experiment.

The substrate and metabolite diffusion coefficients in the membrane ($D_{mem,sub}$ and $D_{mem,met}$) are found by multiplying the estimated aqueous diffusion coefficient (7.5×10^{-6} cm^2/s) by a multiplication factor which accounts for membrane volume fraction and tortuosity and has been reported to be 0.2 for the polycarbonate membrane used in these experiments.[10]

Table 1 shows the various constants and their values used in the model to predict E_d values for phenacetin and acetaminophen and their probe outlet metabolite concentration. All diffusivity and kinetic rate constant model values for acetaminophen and phenacetin were identical except for the estimated metabolic rate constant, k_m. The phenacetin rate constant was evaluated from its microsomal clearance (a measure of metabolism) reported as 33 mL/min/mg microsomal protein, and then multiplied by a constant 45 mg protein/g liver.[32] This product was then multiplied by an estimate of the liver density of 1.2 g/mL to obtain the estimated phenacetin k_m value of 1.8 min^{-1}. In vivo disposition predictions from microsomal data have been previously described.[33]

K_m and V_{max} values for acetaminophen sulfation and glucuronidation have been reported to be 10 μM, 500 nmol/min/liver, and 200 μM, 1000 nmol/min/liver, respectively.[18] These data are estimated from perfused liver experiments which used flow rates of 10 mL/min. V_{max} in units of μM/min becomes 50 μM/min for sulfation and 100 μM/min for glucuronidation. Assuming the concentration of the substrate is less than K_m, the substrate metabolism rate constant, $k_{m,sub}$ found by using the ratio V_{max}/K_m, reduces to 5.0 min^{-1} for sulfation and 0.5 min^{-1} for glucuronidation. The k_{ep} for both drugs and their metabolites was estimated to be 2.0 min^{-1}, which is the estimated flow limited value for a high-clearance drug such as acetaminophen.[34]

Microdialysis—CMA-10 microdialysis probes with an exposed 4 mm polycarbonate membrane (i.d. 400 μm, o.d. 500 μm), (CMA/Microdialysis, Acton, MA) and outlet tubing cut to a length of 3 cm were used for liver experiments with a perfusion flow rate of 1.0 mL/min with a Ringer's solution containing 147 mM NaCl, 4 mM KCl, and 2.3 mM $CaCl_2$. Prior to use, the probes were rinsed with ethanol to remove the glycerol used in the manufacturing process. The recovery is determined by using eq 1 with the value of $C_{\infty ECF}$ set to zero.

Preparatory Surgical Procedures—Male Sprague–Dawley rats (220–280 g) were obtained from a local breeding colony at the University of Kansas. Rats were anesthetized with 200 mg/kg ketamine and 15 mg/kg xylazine, im. All animal experimental procedures were approved by the local ethical committee at the University of Kansas. Rats were allowed food and water ad libitum and were on a 12 h on/off lighting cycle. The core temperature of the animal was maintained at 37 °C by using a CMA/150 temperature monitor (CMA/Microdialysis AB, Stockholm, Sweden) during all experiments.

Microdialysis Probe Implantation—The details of the microdialysis probe implantation have been previously described.[15] Briefly, the liver was exposed by making an incision perpendicular to the midline of the animal approximately 1 cm from the xyphoid process. The lower lobe (right) was then secured to the abdominal wall by a suture through the skin and lobe. This prevented excessive movement of the liver lobe. A second suture was then prepared to secure the microdialysis probe. A 23-gauge needle was used to gently pierce the outside of the liver tissue to allow for careful insertion of the dialysis probe through this hole toward the head and parallel to the midline. The cannula was secured to the skin by a third suture to prevent excessive probe movement during respiration. A large piece of tape was used to cover the incision to prevent tissue dehydration.

After probe insertion, a wash-out period of 1 h was used to clear the ECF space of substances released due to cellular damage caused by the implantation procedure. After the wash-out period, samples were collected every 15 min using a perfusion rate of 1 μL/min. A puncture wound accompanies the implantation of the microdialysis probe; however, previous histology studies for microdialysis in the liver indicate that once the microdialysis probe is implanted the tissue area around the microdialysis probe is in intimate contact with the microdialysis probe.[35]

Dialysate blanks were collected for 1 h prior to changing the perfusion fluid with a liquid switch (CMA-111, CMA/Microdialysis AB, Stockholm, Sweden) to the phenacetin (60 μM) or acetaminophen solutions (12, 120, and 240 μM). The dialysates were analyzed for total phenacetin and its metabolites acetaminophen and acetaminophen sulfate. Measuring phenacetin, acetaminophen, and acetaminophen sulfate in the same chromatographic run was found to be impractical because phenacetin is much more highly retained than acetaminophen. A gradient chromatographic system was not available to alleviate the problem of phenacetin having a retention time of greater than 2 h with the isocratic chromatographic conditions necessary to resolve acetaminophen from acetaminophen sulfate. For this reason and because the model as currently formulated does not provide for the sequential metabolism observed with phenacetin, a second set of experiments using acetaminophen in the perfusion fluid were performed.

LC Analyses—A Shimadzu LC-6A pump was used with a Shimadzu variable wavelength detector set to 254 nm. A Phenomenex (Torrence,CA) C-8 spherex 3 mm column (150 mm × 2.0 mm(i.d.)) was used at a flow rate of 0.22 mL/min. A mobile phase consisting of 97/3 (v/v%) 0.5 M sodium phosphate pH 2.7 and acetonitrile was used. An underfill injection of 7 μL was performed manually with a syringe that had a Cheney adapter. Standard curves were prepared using phenacetin, acetaminophen, acetaminophen sulfate and acetaminophen glucuronide.

Chemicals—Phenacetin, acetaminophen, and acetaminophen glucuronide were obtained from Sigma (St.Louis, MO). Acetaminophen sulfate was a gift from the McNeil Consumer Products Co. (Ft. Washington, PA). Ketamine and xylazine were obtained from the local animal care facility at the University of Kansas.

Results and Discussion

The amount of phenacetin lost from the microdialysis probe at 1.0 μL/min along with the concentration of acetaminophen and acetaminophen sulfate gained back into the perfusion fluid is shown in Table 2 and Figure 2 for an individual rat. A steady-state loss of phenacetin and gain of the metabolites was approached within 45 min as shown in Table 2. At steady-state, approximately 10% of the total concentration of phenacetin lost was recovered as either the converted acetaminophen or acetaminophen sulfate metabolite. The 10% recovered conversion of the phenacetin metabolites will be termed the metabolite fraction, $M_{fraction}$, for clarity. Phenacetin eluted 2 h after acetaminophen with the chromatographic conditions necessary to resolve acetaminophen from acetaminophen sulfate. The rapid conversion of acetaminophen to acetaminophen sulfate after delivery of phenacetin complicated the model analysis originally intended for these experiments. The

Table 2—Phenacetin (60 μM) Delivery to a Rat at 1.0 μL/min[a]

time (min)	[phenacetin], μM, lost from probe	[APAP-SO_4], μM gained	[APAP], μM gained	total APAP metabolites (μM)	$M_{fraction}$
15	15.4	0.38	1.06	1.44	9.35
30	23.6	0.79	1.58	2.37	10.04
45	28.7	1.29	1.42	2.71	9.44
60	27.7	0.99	1.59	2.58	9.31
75	29.1	1.21	1.51	2.72	9.35
90	25.5	1.06	1.89	2.95	11.6
model results	[phenacetin], μM, lost from probe		[APAP], μM gained		$M_{fraction}$
$k_{ep,met}$, $k_{ep,sub}$ = 2.0 min^{-1}	24.46		5.78		23.6
$k_{ep,met}$, $k_{ep,sub}$ = 5.0 min^{-1}	25.72		3.29		12.8

[a] Recovery of the metabolites acetaminophen and acetaminophen sulfate are reported in μM. Each sample represents a collection time of 15 min, which began after the collection of blanks for 1 h. The model predictions for two different $k_{ep,met}$ and $k_{ep,sub}$ values are listed below the experimental results. The other parameters used in this model prediction are listed in Table 1.

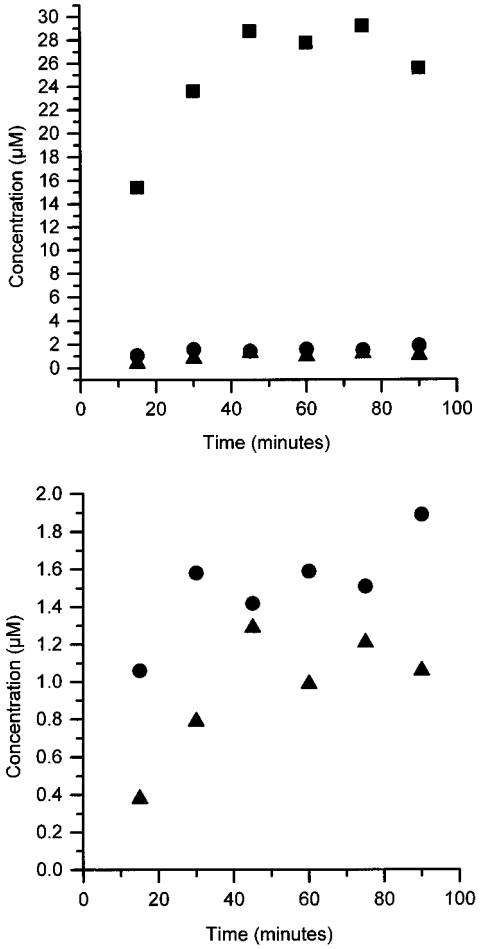

Figure 2—Concentration-time profile for the *loss* of phenacetin (■) and the *gain* of acetaminophen (●) and acetaminophen sulfate (▲) into the microdialysis probe, which was perfused at 1.0 μL/min; 60 μM phenacetin was included in the perfusion fluid. The graph on the bottom shows an enlarged baseline for the graph on the top. Note that the concentration plotted is the concentration exiting the probe at the collection time point and is not averaged across the collection time as is usually the case for microdialysis pharmacokinetic studies.[45]

model as presently formulated cannot predict concentrations of multiple metabolite formation. Although possible to do, the additional computer programming required was not done because the experiments were not designed for such an analysis. To model the formation of multiple metabolites after a local microdialysis delivery of a substrate would require inclusion of a metabolic model such as that described by Morris and Pang to calculate multiple metabolites generated from liver perfusion studies into the microdialysis model.[36]

Table 3—Metabolite Recovery from a Local Infusion of Acetaminophen for Three Separate Rats

[APAP], μM (C_{inlet})	[APAP], μM $[S]_{lost}$ (±SD)	mean E_d, [APAP] (%) (±SD)	$[AS]_{gain}$, μM (±SD)	$M_{fraction}$[a]
		Rat 1		
11.9 (A)	3.7 ± 0.5	31.1 ± 4.2	0.40 ± 0.026	10.82
119 (B)	35.6 ± 4.9	29.9 ± 4.1	2.34 ± 0.03	6.59[c]
238 (C)	61.4 ± 6.0	25.8 ± 2.5	3.54 ± 0.14	5.77[d]
		Rat 2		
11.9 (A)	3.4 ± 0.1	28.6 ± 0.8	0.22 ± 0.12	6.25
119 (B)	27.4 ± 2.0	23.0 ± 1.7	1.56 ± 0.06	5.69[c]
238 (C)	52.1 ± 5.2	21.9 ± 2.2	2.88 ± 0.2	5.54[d,e]
		Rat 3		
11.0 (A)	1.8 ± 0.2	16.3 ± 1.8	0.16 ± 0.02	9.53
110 (B)	18.9 ± 1.5	17.2 ± 1.4	1.03 ± 0.15	5.44[c]
220 (C)	49.8 ± 4.4	22.6 ± 2.0	1.57 ± 0.55	3.17[d,e]
		Model[f]		
100 (1)	23.6	23.6	5.08	21.5
100 (2)	25.1	25.1	2.80	11.2

[a] The $M_{fraction}$ is found by multiplying the ratio of $[AS]_{gain}/[APAP]_{lost}$ by100. [b] Probes were perfused at 1.0 μL/min with acetaminophen in three different rats starting with the lowest concentration (11–12 μM, group A). The solution was changed to the higher acetaminophen concentrations (110–120 μM, group B, and 220–240 μM, group C) by using a liquid switch. A 15 min wash–out period was used between each concentration change. Data are expressed as mean ± standard deviation (n = 4 for each concentration in one rat). [c] There is no statistical difference between the percentage recovered between groups A and B using a paired t-test. [d] (P < 0.1) by using a paired t-test between groups A and C. [e] There is no statistical difference in the percentage recovered between groups B and C. [f] Models 1 and 2 included the parameters listed in Table 1 with $k_{ep,met}$ and $k_{ep,sub}$ =2.0 and 5.0, $k_{m,apap}$ = 1.4 as estimated using sulfate data from Table 4. Diffusion parameters are as listed in Table 1.

The $M_{fraction}$ for acetaminophen sulfate when acetaminophen was perfused through the probe is lower than that of phenacetin and is shown in Table 3 and Figure 3. This is most likely due to differences in the in vivo transport properties of acetaminophen as compared to acetaminophen sulfate. Despite the high capillary exchange rates in liver, metabolites can be recovered after a local infusion of phenacetin or acetaminophen. No acetaminophen glucuronide metabolite was detected during the infusion of acetaminophen.

There are several explanations for the lack of acetaminophen glucuronide in the dialysate after infusion of acetaminophen through the microdialysis probe. The primary explanation is that glucuronides typically are released into the bile duct after formation since the glucuronyltransferases are membrane-bound. On the basis of this argument, any acetaminophen glucuronide formed will be excreted into the bile duct. Glucuronides of phenol have been detected in vivo in the bile by Scott and Lunte[37] and Davies and Lunte after iv injection of phenol.[4] In

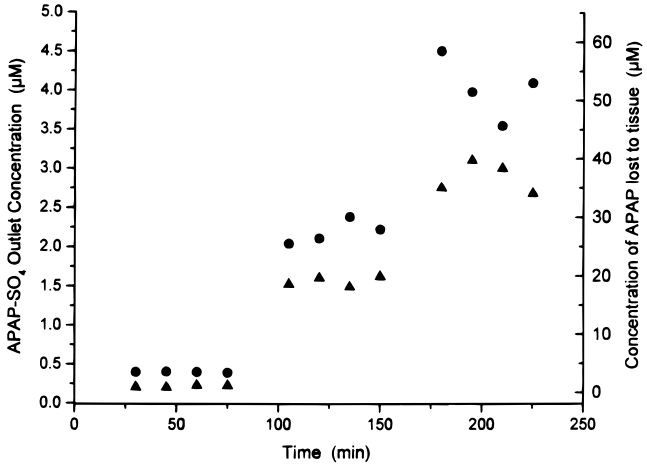

Figure 3—Concentration time profile for the *gain* of acetaminophen sulfate (APAP–SO_4) (▲) and the loss of acetaminophen (APAP) (●) when APAP was perfused through the probe (1.0 μL/min) at concentrations of 11, 110, and 220 μM. The perfusion fluid concentration was changed at 75 and 150 min.

Table 4—Estimates of Michaelis–Menten Parameters for Phenolic Conjugation in a Perfused Liver Model[a]

solute	K_m (sulfate) (μM)	V_{max} (sulfate) (nmol/min)	K_m (glucuronide) (μM)	V_{max} (glucuronide) (nmol/min)
Phenolic Model Drug	10	500	200	1000
Acetaminophen	109	1476	915	828

		model A		model B	
solute	input liver concn (μM)	% sulfate	% glucuronide	% sulfate	% glucuronide
phenolic model	1	90.1	9.4	99.3	0.29
	10	86.4	12.6	98.2	0.71
	50	66.6	21.4	73.5	10.0
	100[b]	42.8	24.0	44.2	18.7
acetaminophen	1	71.5	4.8	72.4	2.4
	10	69.9	4.9	65.2	3.0
	50	63.1	5.3	56.6	3.6
	100	55.1	5.6	43.1	4.4
	200	42.3	5.8	28.0	4.8

[a] Based on the liver perfusion modeling work of Morris and Pang.[36] Model A assumes homogeneous distribution of enzymes. Model B assumes that sulfotransferases are encountered along the sinusoid before glucuronyltransferases. Note that these acetaminophen data were not found in the literature until after most of the simulations in this paper were performed. Therefore, all the simulations use the estimate for sulfation and glucuronidation based on Pang's model phenolic substrate data. [b] 200 μM was not calculated for the phenolic model substrate in the paper by Morris and Pang.

addition to the majority of glucuronide products being excreted into the bile duct, the efflux of acetaminophen glucuronide out of hepatocytes is lower than for acetaminophen sulfate. Iida et al. report that in incubations of hepatocytes with 5 mM acetaminophen in the media, efflux of acetaminophen glucuronide is approximately 4 nmol/10^6 cells, whereas acetaminophen sulfate efflux is 10 nmol/10^6 cells, indicating a 2.5-fold preference for the sulfate conjugate.[38]

Another explanation for the lack of acetaminophen glucuronide collection into the dialysate after acetaminophen perfusion may be related to the enzyme kinetics for the production of these metabolites. Table 4 shows data obtained from perfused rat liver models performed by Morris and Pang.[36] The kinetic parameters for a model phenolic sulfotransferase and glucuronyltransferase are compared to that of estimates for acetaminophen metabolism. The data shown are for different concentration inputs

Table 5—Modeling Predictions of the Changes in $M_{fraction}$ with Changes in the Metabolite Diffusion Coefficient, $D_{ECF,met}$, and Capillary Permeability, $k_{ep,met}$[a]

$D_{ECF,met}$ (cm^2/s)	$D_{mem,met}$ (cm^2/s)	Φ_{ECF}	$k_{ep,met}$	$[S]_{lost}$ (μM)[b]	M_{gain} (μM)	$M_{fraction}$
3.33×10^{-6}	7.5×10^{-6}	0.2	2.0	2.8	0.852	30.4
		0.2	1.0	2.8	1.035	37.0
		0.2	0.5	2.8	1.202	42.9
2.97×10^{-6}	7.5×10^{-6}	0.2	2.0	2.8	0.861	30.8
		0.2	1.0	2.8	1.046	37.4
		0.2	0.5	2.8	1.216	43.4
2.97×10^{-6}	6.75×10^{-6}	0.2	2.0	2.8	0.840	30.0
		0.2	1.0	2.8	1.025	36.6
		0.2	0.5	2.8	1.195	42.7
2.64×10^{-6}	6.0×10^{-6}	0.2	2.0	2.8	0.823	29.4
		0.2	1.0	2.8	1.001	35.8
		0.2	0.5	2.8	1.183	42.3
3.33×10^{-6}	7.5×10^{-6}	0.4	2.0	2.8	0.714	25.5
		0.4	1.0	2.8	0.932	33.3
		0.4	0.5	2.8	1.153	41.2

[a] The model was performed using the acetaminophen parameters listed in Table 1 with an initial concentration of 10 μM. The in vivo and membrane diffusion coefficients listed in Table 1 were reduced 10% and 20% to achieve the reduced diffusion coefficients in columns 1 and 2. [b] The E_d for the substrate in all cases was 28.3% assuming a $D_{ECF,Sub}$ of 3.3×10^{-6} cm^2/s.

for a perfused liver model (model A) that assumes homogeneous distribution of these two enzymes. The numbers do not sum to 100% because the extraction efficiency of the liver removal is also included in Pang's models. For the model phenolic compound, approximately 43% is predicted to be converted into a sulfate metabolite, while 25% is predicted to become a glucuronide. The results for acetaminophen show that approximately 5% of the dose would become a glucuronide metabolite in a system with an assumption of homogeneous distribution of enzymes. It is known that in the hepatocytes homogeneous distribution does not occur and so a more appropriate model would be that of model B, which assumes the drug first passes through a zone containing sulfotransferases only and then passes through a zone that only contains glucuronyltransferases. For this model simulation, which is closer to the in vivo reality, the conversion of acetaminophen to its glucuronide ranges between 2.2% and 4.4%. With such low conversion rates, it is unlikely that a detectable amount of acetaminophen glucuronide could have entered the dialysate.

Table 5 shows the affect on E_d of a lower metabolite in vivo diffusion coefficient, membrane diffusion coefficient, and $k_{ep,met}$. Diffusion coefficients were lowered by 10% and 20% as an estimate in the change in diffusion coefficient due to changes in molecular weight differences of the metabolite. Using a Stokes−Einstein relationship as an approximation to calculate the differences between substrate and metabolite in vivo and membrane diffusion coefficient because of molecular weight change, the expected change in diffusion coefficients would be based on the cubed root of the molecular weight.[39] The difference between the parent compound acetaminophen (MW 151) and the metabolites acetaminophen sulfate (MW 231) and acetaminophen glucuronide (MW 326) would be an approximate 15% and 30% reduction in the diffusion coefficient based on the approximate Stokes−Einstein relationship. The lowering of the metabolite in vivo diffusion coefficient by 10% of the parent in vivo diffusion coefficient while keeping $D_{mem,met}$ and $k_{ep,met}$ the same as the parent compound increases the $M_{fraction}$ slightly. A 10% decrease in both the in vivo and membrane diffusion coefficient decreases $M_{fraction}$. A 20% decrease in both the in vivo and membrane diffusion coefficient only makes about a 1% change in the $M_{fraction}$. Table 5 clearly shows that $M_{fraction}$ is more highly dependent upon the metabolite capillary

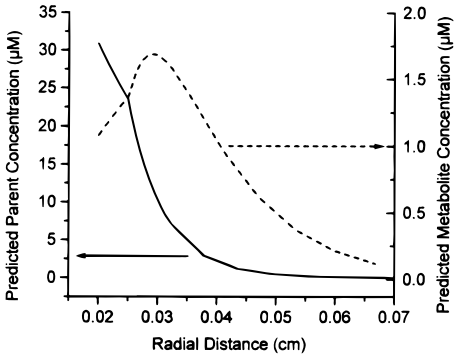

Figure 4—Model prediction of the concentration profile in the tissue space for the substrate (solid line pointing to the left axis) and the metabolite (dashed line pointing to the right axis).

permeability, $k_{ep,met}$, rather than in vivo and membrane diffusion coefficients.

To quickly determine the diffusion coefficient differences between acetaminophen and its metabolites an in vitro recovery (stirred) of acetaminophen, acetaminophen sulfate, and acetaminophen glucuronide was performed. The recoveries found using a perfusion rate of 1.0 μL/min at 23 °C were 49%, 42%, and 28% for acetaminophen, acetaminophen sulfate, and acetaminophen glucuronide, which clearly indicates that acetaminophen glucuronide has a lower aqueous diffusion coefficient than acetaminophen or acetaminophen sulfate. Using the resistance equations derived by Bungay et al.,[10] the reduction in solution diffusion coefficient between acetaminophen and its metabolites is 19% (sulfate) and 51% (glucuronide) based on these in vitro E_d values. With a lower effective diffusivity through the dialysis membrane, it is expected that acetaminophen glucuronide would also have a lower tissue diffusivity and possibly a lower in vivo extraction efficiency than acetaminophen sulfate. The in vivo recovery of acetaminophen was approximately 25%, as shown in Table 3. The in vivo recoveries of acetaminophen sulfate and acetaminophen glucuronide would be expected to be lower than acetaminophen because they have lower diffusion coefficients and because they do not undergo further metabolism, thus reducing the contribution of kinetic processes to k_L in eq 2, which would have the effect of decreasing the recovery.

The model predicts a $M_{fraction}$ of 21.5% for acetaminophen with a $k_{ep,sub}$ and $k_{ep,met} = 2.0$ min^{-1} and a $M_{fraction}$ of 11.2% for $k_{ep,sub}$, $k_{ep,met} = 5.0$ min^{-1} using the acetaminophen data presented by Morris and Pang.[40] These data are shown in Table 3 for comparison with the experimental data for acetaminophen. The model predicts a $M_{fraction}$ of 23.6% for phenacetin conversion to acetaminophen using $k_{ep,sub}$ and $k_{ep,met} = 2.0$ min^{-1} and 12.8% for $k_{ep,sub}$, $k_{ep,met} = 5.0$ min^{-1}. The metabolite recovery obtained for the metabolites of phenacetin and acetaminophen do not match the model predictions using the k_{ep} flow limited estimate of 2.0 min^{-1},[34] but they are not worse than a factor of 2−3, which is not unexpected when a complex model is used to predict events which occur in a complicated biological matrix. Possible reasons for the discrepancy include incorrect estimates of the diffusion and kinetic parameters and/or possible convection around the microdialysis probe. The diffusion coefficient used in the model prediction was the same for the metabolite as for the parent compound. Additionally it is possible that capillary permeation may be different between the parent and metabolite. A decrease in the k_L that describes total metabolite kinetic processes would allow more of the metabolite to enter the probe, as shown in Table 5 for various changes in k_{ep}. Thus, $M_{fraction}$ for any metabolite will be dependent upon metabolite kinetic and diffusive properties in the tissue.

Table 6—Modeled Metabolite Concentration Differences between Linear and Michaelis–Menten Metabolism[c]

C_{inlet} [S] (μM)	modeled recovery (%)	C_{outlet} [S]	lost across membrane/ (pmol/min)	$[M]_{gain}$, outlet	$M_{fraction}$
1.0 (linear)[a]	28.7	0.71770	0.287	0.085	29.7
1.0 (MM)[b]	28.7	0.71770	0.287	0.084	29.3
10.0 (linear)	28.7	7.1770	2.87	0.85	29.7
10.0 (MM)	28.7	7.1770	2.87	0.75	26.0
100.0 (linear)	28.7	71.770	28.7	8.5	29.7
100.0 (MM)	28.7	71.770	28.7	3.9	13.5
200.0 (linear)	28.7	143.54	57.4	17.1	29.7
200.0 (MM)	28.7	143.54	57.4	5.3	9.3

[a] Indicates that the amount of metabolite predicted to enter into the probe was calculated by using the model which assumes linear metabolism and that C_{ECF} is lower than K_m for the substrate compound. [b] MM indicates that Michaelis–Menten kinetics were included in the generation term of the metabolite model. [c] Model parameters are as follows: $k_{ep,sub} = 2.0$ min^{-1}, $k_{m,sub,icf} = 5.0$ min^{-1}, $k_{m,met} = 0.0$ min^{-1}, $k_{ep,met} = 2.0$ min^{-1}, $V_{max} = 50$ μM/min, $K_m = 10$ μM. $Q_d = 1.0$ μL/min. [S] and [M] stand for the concentrations of the substrate and metabolite.

Figure 4 shows the predicted metabolite and substrate concentration profiles to and from the microdialysis probe as calculated by the model. The metabolite concentration profile from the probe has a maximum value offset from the phenacetin (subsrate) concentration profile. This occurs because of the concentration gradient caused by removal of material by the microdialysis probe and the sink conditions in the tissue caused by removal processes such as capillary uptake or bile duct removal. The metabolite actually has two directions in which it can move to an area of lower concentration: the probe and the far-field tissue space. The probe acts as an artificial blood vessel that is capable of removing the metabolite from the tissue. Since the concentration of the parent compound is zero at the far-field boundary, the metabolite concentration at that space point would also be expected to be zero. Thus, the far-field boundary is a sink for the metabolite that is generated closer to the probe.

The $M_{fraction}$ for acetaminophen sulfate is statistically different ($P < 0.1$) between the 11 and 220 μM acetaminophen perfusions. This appearance of concentration dependence can be attributed to two factors. The obvious explanation is that the concentration in the ECF using acetaminophen concentrations of greater than 100 μM in the dialysis perfusion fluid may exceed the estimated K_m for the phenolsulfotransferase, which is 10 μM.[21] After the compilation of all the model data, the paper by Morris and Pang was found which contains an estimated K_m for acetaminophen of 109 μM.[36] Using this estimate, the change in $M_{fraction}$ between different concentrations can still be explained by nonlinear Michaelis−Menten kinetics. The second is that the protein that transports acetaminophen sulfate from the intracellular space to the extracellular space may be saturated.[41] A shift would be expected for the values between 10 and 50 μM for the acetaminophen as modeled by Morris and Pang for the isolated perfused liver[36] and described experimentally for phenol and other phenolic compounds by others.[42] Table 6 shows the prediction differences between the model that uses linear kinetics for the production of metabolite versus Michaelis−Menten kinetics. Changes in the $M_{fraction}$ will occur with saturation of enzymes due to the reduction of the enzymatic velocity based on calculations using Michaelis−Menten kinetics.

Other authors have reported the formation and collection of metabolites from microdialysis experiments in rat liver. Van Belle et al. observed an $M_{fraction}$ of 18% for oxidative

Table 7—$M_{fraction}$ Predictions for Different $k_{ep,met}$[a]

$k_{ep,met}$	steady state concn in dialysate	$M_{fraction}$	maximum concn	E_d (est)[a]	C_{dial}/C_{Max}	C_{max} radial position
0.001	18.24	64.5	61.5	5.08	29.7	0.0317
0.01	17.35	61.3	57.6	5.75	30.1	0.0306
0.05	15.92	56.3	51.6	7.43	30.9	0.0301
0.1	15.01	53.0	48.0	8.61	31.7	0.0296
0.5	12.03	42.5	36.9	12.6	32.6	0.0286
1.0	10.36	36.6	31.2	15.0	33.2	0.0280
2.0	8.52	30.1	25.2	17.7	33.8	0.0275
5.0	6.07	21.4	17.6	21.7	34.5	0.0275

[a] Initial substrate concentration was found by using the values listed in Table 1. The modeled substrate recovery was 28.3% using an inlet concentration of 100 μM. In the calculation of the metabolite outflow concentration, $k_{m,met}$ is set to zero. k_{ep} in these simulations was varied and thus not set at 2.0 min^{-1} as shown in the table. [b] E_d (est) is the modeled in vivo E_d for the metabolite based on the parameters in Table 1 and $k_{ep,met}$ given in this table.

conversion of carbamazipine when it was included in the microdialysis perfusion fluid using a 2 μL/min perfusion flow rate.[5] The 18% $M_{fraction}$ of this oxidative metabolite was reported to agree with isolated perfused liver data. They also suggested that microdialysis can be used as an alternative to isolated perfused liver studies to determine the metabolic formation of compounds. In our work acetaminophen produced an $M_{fraction}$ of 4−10% at a perfusion flow rate of 1 μL/min. The acetaminophen data presented here do not match that of isolated perfused liver data, which has reported a 75% conversion of acetaminophen to acetaminophen sulfate at concentrations entering the perfused rat liver of less than 40 μM.[43] There may be several reasons for this discrepancy. First, these animals were anesthetized with ketamine which may interfere with local metabolism. A second reason, which is more likely, is that $M_{fraction}$ is a function of physiological parameters for the metabolite and probe parameters such as membrane length and flow rate.

Table 7 and Figure 5 exhibit the model predictions and concentration profiles for variations in $k_{ep,met}$. Table 7 shows that $C_{dialysate,met}$ and $M_{fraction}$ will increase as $k_{ep,met}$ decreases for a substrate with model parameters listed in Table 1 for acetaminophen. This table also shows the metabolite maximum concentration and its corresponding radial point in the ECF. The position of the maximum concentration does not change more than 50 μm between a $k_{ep,met}$ of 0.001 min^{-1}, which would be poor capillary permeability, and a $k_{ep,met}$ of 5.0 min^{-1}, which would be high capillary permeability. This small change in the maximum concentration radial position shows that the probe is sampling from a limited area.

A ratio of C_{dial} divided by this maximum concentration is shown in Table 7 for each $k_{ep,met}$ value. This ratio can be compared to a model-predicted E_d for the metabolite based on the $k_{ep,met}$ values given. These model predictions show that an in vivo E_d for the metabolite cannot be used to predict the maximum concentration in the tissue. The concept of E_d is based on knowing C_{sample} and C_{dial} for an unknown. For a recovery experiment, C_{sample} is the far-field concentration and C_{dial} is zero, whereas for a delivery experiment C_{sample} is set to zero and C_{dial} is known. In these metabolism experiments, C_{sample} varies across the ECF and is zero at the far field but reaches a maximum at distances that vary from the probe center based on the metabolite physiological parameters. The probe is sampling a space very close to it and is removing very little material. This removal does not appear to affect the maximum concentration distance significantly, which means that little is being removed. The lack of change in C_{sample} for a recovery

Table 8—Effect of Q_d on $M_{fraction}$[a]

flow rate (μL/min)	C_{outlet}	E_d (substrate)	$C_{metab,outlet}$	C_{Max}	E_d (est)	C_{dial}/C_{max}	C_{max} position
0.5	55.9	44.1	11.3	22.13	30.0	0.51	0.0275
1.0	71.7	28.3	8.5	25.22	17.7	0.34	0.0275
2.0	83.5	16.5	5.5	27.12	9.7	0.20	0.0280
5.0	92.7	7.3	2.6	28.38	4.1	0.09	0.0280

[a] The model was calculated using k_m = 5.0 min^{-1} and k_{ep} = 2.0 min^{-1}.

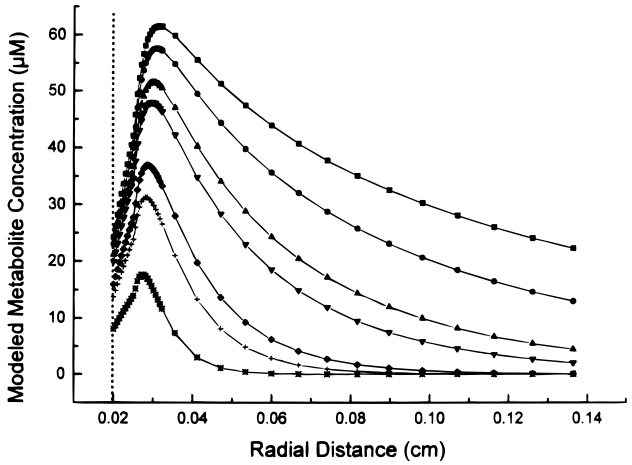

Figure 5—Model predicted concentration profiles with varying values of capillary permeation, k_{ep}. k_{ep} = 0.001 (■), 0.01 (●), 0.05 (▲), 0.1 (▼), 0.5 (◆), 1.0 (+), and 5.0 (*). The dashed line indicates the position of the membrane.

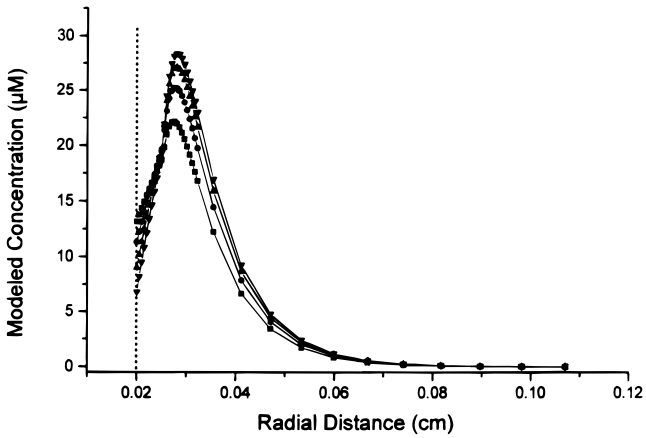

Figure 6—Model predicted concentration profiles with different values of the volumetric flow rate, Q_d: (■) 0.5 μL/min, (●) 1.0 μL/min (▲), 2.0 μL/min (▼), 5.0 μL/min. The dashed line indicates the position of the membrane.

experiment of dopamine has been reported with flow rates varying between 0.3 and 1.6 μL/min, where no change in C_{sample} was observed.[44] Table 7 shows that with decreasing E_d, $M_{fraction}$ will increase.

Table 8 and Figure 6 shows the affect of using different Q_d in the calculation of $M_{fraction}$. $M_{fraction}$ increases with decreasing Q_d. This may be due to more mass being collected at the higher flow rates. More mass is released per minute at the higher flow rates and more mass is gained back. Additionally, probe residence time may affect $M_{fraction}$ since a metabolite in the perfusate could diffuse back into the tissue space if time and concentration gradients conditions exist to permit back-diffusion into the ECF to occur. This indicates that comparing microdialysis results for the conversion of a metabolite to liver perfusion data is highly dependent upon the conditions of the experiment such as flow rate and membrane length plus

Table 9—Effect of Membrane Length on Modeled Results[a]

length (mm)	E_d(substrate)	$[M]_{dial}$	$M_{fraction}$	E_d(metabolite)
1	9.0	3.1	34.4	5.1
2	16.5	5.4	32.7	9.7
4	28.3	8.5	30.0	17.7
10	49.6	11.8	23.8	35.0

[a] The model parameters are listed in Table 1. $k_{m,sub} = 5.0$ min^{-1}. E_d(metabolite) is calculated using the parameters in Table 1 with $k_{m,met} = 0.0$ min^{-1}.

the physiological parameters of metabolism rate constant and capillary permeability.

Our proportion of $M_{fraction}$ results also differ from those of Davies and Lunte.[4] They report hydroquinone concentrations between 0.62 and 5.8 μM after a 100% E_d loss of phenol to the liver. These results give $M_{fraction}$ of less than 1%, which is lower than what we observe for acetaminophen and phenacetin. With such a high E_d, it is possible that any metabolite that diffused into the probe at one point along the probe axis may then diffuse out again further down the probe axis. Table 9 shows that with increasing length, and thus increasing E_d, the $M_{fraction}$ decreases. This is likely due to back-diffusion of the metabolite into the ECF space. Thus, the variation in E_d due to physiological parameters, volumetric flow rate, and membrane length will greatly affect the results obtained when using microdialysis to study in situ metabolism.

Summary

In the present study it has been demonstrated that microdialysis can be used to study local metabolism in the liver when a substrate compound is included in the perfusion fluid. Substrates metabolized through cytochrome P450 processes and conjugation processes can be subject to such studies. However, not all possible metabolites may enter the microdialysis probe because of physicochemical, physiological, and/or mass transport reasons such as was shown with the lack of acetaminophen glucuronide after acetaminophen perfusion. The mathematical model was used to predict the concentrations of metabolites produced after one-step metabolism of a substrate delivered from a microdialysis probe. Predictions of $M_{fraction}$ are dependent upon metabolite physiological and microdialysis probe parameters. Further work is necessary to develop the model to be able to predict concentrations from processes which occur via multistep metabolic pathways.

Glossary

C_{outlet}	Outlet concentration from the microdialysis probe (mol/L; M)
C_{inlet}	Inlet concentration into the dialysis probe (mol/L; M)
$C_{\infty ECF}$	Far-field concentration (mol/L; M)
$C_{ECF}(r,t)$	Concentration of any species in the ECF at position r and time t (mol/L; M)
$D_{mem,sub}$	Membrane diffusion coefficient for the substrate (cm^2/s)
$D_{mem,met}$	Membrane diffusion coefficient for the metabolite (cm^2/s)
$D_{ECF,sub}$	ECF diffusion coefficient for the substrate (cm^2/s)
$D_{ECF,met}$	ECF diffusion coefficient for the metabolite (cm^2/s)
E_d	Recovery (extraction fraction) (dimensionless)
G_i	Generation term of the metabolite in the tissue space (M/min)
$k_{ep,met}$	Capillary permeability rate constant (metabolite) (min^{-1})
$k_{ep,sub}$	Capillary permeability rate constant (substrate) (min^{-1})
$k_{m,met}$	Metabolism rate constant (metabolite) (min^{-1})
$k_{m,sub}$	Metabolism rate constant (substrate) (min^{-1})
k_L	Lumped kinetic term (min^{-1})
K_m	Michaelis constant (mol/L; M)
$[M]_{dial}$	Absolute metabolite concentration exiting the dialysate (mol/L; M)
$M_{fraction}$	$[M]_{dial}/[S]_{lost}$ (dimensionless)
Φ_{ECF}	Volume fraction in the ECF (dimensionless)
Φ_{mem}	Volume fraction in the membrane (dimensionless)
Q_d	Dialysate volumetric flow rate (cm^3/min)
r	Radial position (cm)
$[S]_{lost}$	$C(\text{substrate})_{inlet} - C(\text{substrate})_{outlet}$ (mol/L; M)
t	Time (min)
V_{max}	Maximum velocity of an enzyme (mol/min)

References and Notes

1. Robinson, T. E.; Justice, J. B., Jr., Eds. *Microdialysis in the Neurosciences*; Elsevier: Amsterdam, 1991.
2. Ungerstedt, U. Microdialysis—Principles and applications for studies in animals and man. *J. Internal. Med.* **1991**, *230*, 365−373.
3. Lunte, S. M.; Lunte, C. E. Microdialysis sampling for pharmacological studies: HPLC and CE analysis. In *Advances in Chromatography*; Brown P. R., Grushka, E., Eds.; Marcel Dekker Inc.: New York, 1996; Vol. 36, pp 383−432.
4. Davies, M. I.; Lunte, C. E. Simultaneous microdialysis sampling from multiple sites in the liver for the study of phenol metabolism. *Life Sci.* **1996**, *59*, 1001−1013.
5. Van Belle, K.; Sarre, S.; Ebinger, G.; Michotte, Y. Brain, liver, and blood distribution kinetics of carbamazepine and its metabolic interaction with clomipramine in rats: A quantitative microdialysis study. *J. Pharmacol. Exp. Ther.* **1995,** *272*, 1217−1222.
6. Scott, D. O.; Lunte, C. E. In vivo microdialysis sampling in the bile, blood, and liver of rats to study the disposition of phenol. *Pharm. Res.* **1993,** *10*, 335−342.
7. Ståhle, L.; Segersvärd, S.; Ungerstedt, U. Drug distribution studies with microdialysis. II. Caffeine and theophylline in blood, brain, and other tissues in rats. *Life Sci.* **1991**, *49*, 1843−1852.
8. Ungerstedt, U; Herrera-Marschitz M; Jungnelius, U; Ståhle, L; Tossman, U.; Zetterström, T. Dopamine synaptic mechanisms reflected in studies combining behavioral recordings and brain dialysis. In *Advances in Dopamine Research;* Kohsaka, M., Ed.; Pergamon Press: New York, 1982; pp 219−231.
9. Ault, J. M.; Riley, C. M.; Meltzer, N. M.; Lunte, C. E. Dermal microdialysis sampling in vivo. *Pharm. Res.* **1994**, *11*, 1631−1639.
10. Bungay P. M.; Morrison P. F.; Dedrick R. L. Steady-state theory for quantitative microdialysis of solutes and water in vivo and in vitro. *Life Sci.* **1990**, *46*, 105−119.
11. Morrison, P. F.; Bungay, P. M.; Hsiao, J. K.; Mefford, I. V.; Dykstra, K. H.; Dedrick, R. L. Quantitative microdialysis. In *Microdialysis in the Neurosciences*, Robinson, T. E., Justice, J. B., Jr., Eds.; Elsevier: Amsterdam, 1991; pp 47−80.
12. Dykstra, K. H.; Arya, A.; Arriola, D. M.; Bungay, P. M.; Morrison, P. F.; Dedrick, R. L. Microdialysis study of zidovudine (AZT) transport in rat brain. *J. Pharmacol. Exp. Ther.* **1993**, *267*, 1227−1236.
13. Wallgren, F.; Amberg, G.; Hickner, R. C.; Ekelund, U.; Jorfeldt, L.; Henriksson, J. A mathematical model for measuring blood flow in skeletal muscle with the microdialysis ethanol technique. *J. Appl. Physiol.* **1995**, *72*, 648−659.

14. Hickner, R. C.; Ekelund, U.; Mellander, S.; Ungerstedt, U.; Henriksson, J. Muscle blood flow in the cat: comparison of the microdialysis ethanol technique to direct measurement. *J Appl. Physiol*. **1995**, *79*, 638−647.
15. Stenken, J. A.; Lunte, C. E.; Southard, M. Z.; Ståhle, L. Factors that influence microdialysis recovery. Comparison of experimental and theoretical microdialysis recoveries in rat liver. *J. Pharm. Sci*. **1997**, *86*, 958−966.
16. Rappaport, A. M. The structural and functional unit in the human liver (liver acinus). *Anat. Rec.* **1958**, *130*, 673−689.
17. Arias, I. M.; Jakoby, W. B.; Popper, H.; Schachter, D., Eds. *The Liver: Biology and Pathobiology*, 2nd ed.; Raven Press Ltd.: New York, 1988.
18. Pang, K. S.; St-Pierre, M. V. Hepatic modeling of drugs and metabolites. In *Biliary Excretion of Drugs and Other Chemicals; Progress in Pharmacology and Clinical Pharmacology*; Siegers, C-P, Watkins, J. B., Eds.; Gustav Fischer Verlag: Stuttgart, 1991; Vol. 8, pp 89−126.
19. Pang, K. S. Kinetics of conjugation reactions in eliminating organs. In *Conjugation Reactions in Drug Metabolism*; Mulder, G. J., Ed.; Taylor and Francis: London, 1990; pp 5−39.
20. Gillette, J. R. Kinetic aspects of metabolism and elimination of foreign compounds in animals. In *Enzymatic Basis of Detoxication*; Jakoby, W. B., Ed.; Academic Press, Inc.: Orlando, 1980; Vol. 1, pp 9−24.
21. Gores, G. J.; Kost, L. J.; LaRusso, N. F. The isolated perfused rat liver: Conceptual and practical considerations. *Hepatology* **1986**, *6*, 511−517.
22. Bass L; Keiding S. Physiologically based models and strategic experiments in hepatic pharmacology. *Biochem. Pharmacol.* **1988**, *37*, 1425−1431.
23. Smith, R. L.; Timbrell, J. A. Factors affecting the metabolism of phenacetin I. Influence of dose, chronic dosage, route of administration and species on the metabolism of (1-c14-acetyl)phenacetin. *Xenobiotica* **1974**, *4*, 489−501.
24. Miner, D. J.; Kissinger, P. T. Evidence for the involvement of *N*-acetyl-*p*-quinoneimine in acetaminophen metabolism. *Biochem. Pharmacol*. **1979**, 3285−3290.
25. Van Belle K.; Sarre S.; Ebinger G.; Michotte Y. Quantitative microdialysis for the in vivo measurement of carbamazepine, oxcarbazepine and their major metabolites in rat brain and liver tissue and in blood using the internal standard technique. *Eur. J. Pharm. Sci.* **1995**, *3*, 273−280.
26. Stenken, J. A. *Identification and Modeling of Parameters that Influence Microdialysis Sampling in vitro and in vivo.* Ph.D. Dissertation, University of Kansas, 1995.
27. Carnahan, B.; Luther, H. A.; Wilkes, J. O. *Applied Numerical Methods*. Robert E. Krieger Publishing: Malabar, FL, 1990.
28. Press, W. H.; Flanner, B. P.; Teukolsky, S. A.; Vetterling, W. T. *Numerical Recipes in FORTRAN: The Art of Scientific Computing*, 2nd ed.; Cambridge University Press: Cambridge, 1986.
29. Laidler, K. J. *Chemical Kinetics*, 3rd ed.; Harper Collins Publishers: New York, 1987; p 401.
30. Rice, M. E.; Gerhardt, G. A.; Hierl, P. M.; Nagy, G.; Adams, R. N. Diffusion coefficients of neurotransmitters and their metabolites in brain extracellular fluid space. *Neuroscience* **1985**, *15*, 891−902.
31. Rice, M. E.; Nicholson, C. Diffusion and ion shifts in the brain extracellular microenvironment and their relevance for voltammetric measurements. The brain is not a beaker: In vivo vs In vitro voltammetry. In *Neuromethods, Vol. 27: Voltammetric Methods in Brain Systems;* Boulton, A., Baker, G.; Adams, R. N., Eds.; Humana Press Inc. New York, 1995; pp 27−79.
32. Houston, J. B. Utility of in vitro drug metabolism data in predicting in vivo metabolic clearance. *Biochem. Pharmacol.* **1994**, *47*, 1469−1479.
33. Hayes, K. A.; Brennan, B.; Chenery, R.; Houston, J. B. In vivo disposition of caffeine predicted from hepatic microsomal and hepatocyte data. *Drug Metab. Disp*. **1995**, *23*, 349−353.
34. Ichikawa, M.; Tsao, S. C.; Lin, Tsu-H.; Miyauchi, S.; Sawada, Y.; Iga, T.; Hanano, M.; Sugiyama, Y. 'Albumin-mediated transport phenomenon' observed for ligands with high membrane permeability: Effect of the unstrirred water layer in the Disse's space of rat liver. *J. Hepatol.* **1992**, *16*, 38−49.
35. Davies, M. I.; Lunte, C. E. Microdialysis sampling for hepatic metabolism studies: Impact of microdialysis probe design and implantation technique on liver tissue. *Drug Metab. Disp.* **1995**, *23*, 1072−1079.
36. Morris, M. E.; Pang, K. S. Competition between two enzymes for substrate removal in liver: Modulating effects due to substrate recruitment of hepatocyte activity. *J. Pharmacokin. Biopharm*. **1987**, *15*, 473−496.
37. Scott, D. O.; Lunte, C. E. In vivo microdialysis sampling in the bile, blood, and liver of rats to study the disposition of phenol. *Pharm. Res*. **1993**, *10*, 335−342.
38. Iida, S.; Mizuma, T.; Sakuma, N.; Hayashi, M.; Awazu, S. Transport of acetaminophen conjugates in isolated rat hepatocytes. *Drug Metab. Disp*. **1989**, *17*, 341−344.
39. Barrow, G. N. *Physical Chemistry*, 5th ed.; McGraw Hill Book Co.: New York, 1988; p 803.
40. The estimated V_{max} and K_m for acetaminophen were found in the paper by Morris and Pang[36] after most of the simulations for the tables were performed using the model phenol metabolism estimates given by Pang.[18]
41. Goresky, C. A.; Pang, K. S.; Schwab, A. J.; Barker, F. I., Cherry, W. F.; Bach, G. G. Uptake of a protein-bound polar compound, acetaminophen sulfate by perfused rat liver. *Hepatology* **1992,** *16*, 173−190.
42. Koster, H.; Halsema, I.; Scholtens, E.; Knippers, M.; Mulder, G. J. Dose-dependent shifts in the sulfation and glucuronidation of phenolic compounds in the rat in vivo and in isolated hepatocytes: The role of saturation of phenolsulfotransferase. *Biochem. Pharmacol.* **1981**, *30*, 2569−2575.
43. Pang K. S.; Terrell J. A. Conjugation kinetics of acetaminophen by the perfused rat liver preparation. *Biochem. Pharmacol.* **1981**, *30*, 1959−1965.
44. Sam, P. M.; Justice, J. B., Jr. Effect of general microdialysis-induced depletion on extracellular dopamine. *Anal. Chem*. **1996**, *68*, 724−728.
45. Ståhle, L. Microdialysis in pharmacokinetics. *Eur. J. Drug Metab. Pharmacokinet.* **1993**, *18*, 89−96.

Acknowledgments

This work was supported by NIH (R01 GM45566) and the Swedish Medical Council (09069). A Procter & Gamble Bioanalytical Chemistry Fellowship and a J. William Fulbright Fellowship to Sweden supported J.A.S. Conversations with Dr. Paul Morrison and discussions, faxes, and e-mail with Dr. Peter Bungay, who both work at the Drug Delivery and Kinetics Resource, Biomedical Engineering & Instrumentation Program, Office of Research Services, National Institutes of Health, are greatly appreciated.

JS970288Z